

Bright cyan fluorescent protein variants identified by fluorescence lifetime screening

Joachim Goedhart^{1,3}, Laura van Weeren^{1,3}, Mark A Hink¹, Norbert O E Vischer¹, Kees Jalink² & Theodorus W J Gadella Jr¹

Optimization of autofluorescent proteins by intensity-based screening of bacteria does not necessarily identify the brightest variant for eukaryotes. We report a strategy to screen excited state lifetimes, which identified cyan fluorescent proteins with long fluorescence lifetimes (>3.7 ns) and high quantum yields (>0.8). One variant, mTurquoise, was 1.5-fold brighter than mCerulean in mammalian cells and decayed mono-exponentially, making it an excellent fluorescence resonance energy transfer (FRET) donor.

Cyan fluorescent protein variants¹ derived from *Aequorea victoria* GFP are widely applied for localization and fluorescence resonance energy transfer (FRET)-based interaction studies^{2,3}. Cerulean and

SCFP3A, which are optimized for folding, are the brightest variants^{4,5}. However, their quantum yields leave room for improvement. So far, screens for improved fluorescent protein variants have been aimed at optimizing the brightness of mutants of these proteins by evaluating the fluorescence intensity in individual bacteria or colonies. However, apart from brightness, colony intensity also reflects expression level, maturation efficiency and thickness of the colony and therefore does not necessarily reflect the brightest variants.

Because for a given fluorophore the quantum yield and the fluorescence lifetime both increase with an increased ratio of radiative to nonradiative decay from the excited state, we devised a fluorescence lifetime-based screen to optimize quantum yield, thereby improving the intrinsic molecular brightness. A major advantage is that the fluorescence lifetime can be determined independently of fluorescence intensity. From such a screen, fluorescent proteins can also be selected for single-exponential decay, which is important for time-resolved FRET measurements.

Our screening setup (Supplementary Fig. 1) was based on a frequency domain fluorescence lifetime imaging microscope⁶, enabling acquisition of a fluorescence lifetime image of an entire Petri dish within seconds from which the fluorescence lifetime (and intensity) of individual bacterial colonies can be determined.

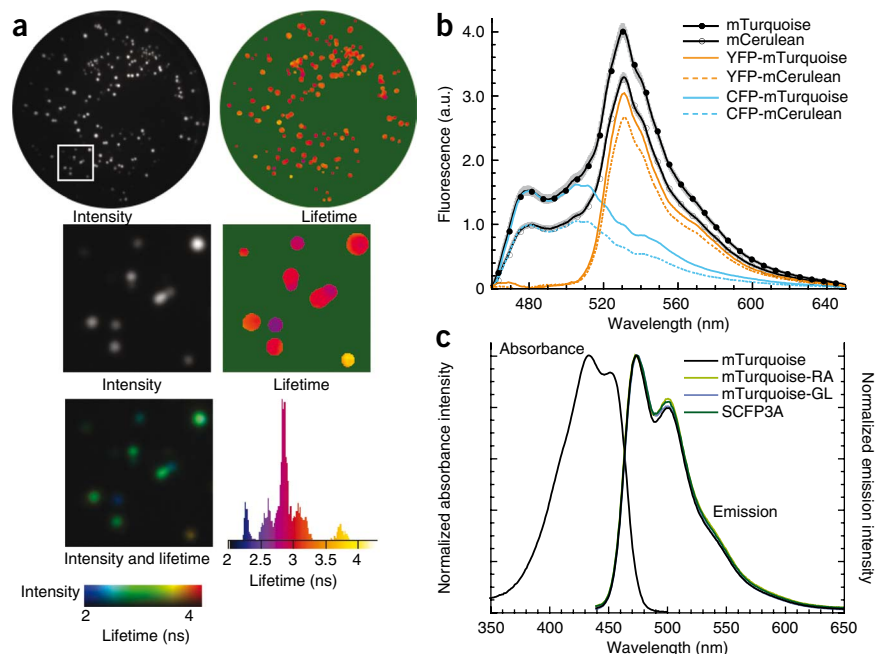


Figure 1 | Fluorescence lifetime screening and spectral properties of cyan fluorescent protein variants. **(a)** Fluorescence intensity and modulation lifetime images of a plate of colonies expressing SCFP3A Thr65 mutants. Boxed region on the plate was magnified for the images below; magnified image width is 14 mm. The lifetimes are false-colored according to the scale in the histogram. **(b)** FRET spectra of mVenus (L68V)-mCerulean ($n = 13$) and mVenus(L68V)-mTurquoise ($n = 14$) with s.e.m. in gray as determined by spectral imaging of living HeLa cells. The FRET spectra were normalized to equal direct excited yellow fluorescence from mVenus(L68V). The cyan and yellow components of the FRET spectra are depicted. **(c)** Absorbance spectrum of mTurquoise and its emission spectrum along with that for mTurquoise-GL, mTurquoise-RA and SCFP3A.

¹Swammerdam Institute for Life Sciences, Section of Molecular Cytology, Centre for Advanced Microscopy, University of Amsterdam, Amsterdam, The Netherlands.

²Division of Cell Biology, The Netherlands Cancer Institute, Amsterdam, The Netherlands. ³These authors contributed equally to this work. Correspondence should be addressed to T.W.J.G. (th.w.j.gadella@uva.nl).

Table 1 | Key properties of cyan fluorescent protein variants

Protein	ϵ ($10^3 \text{ M}^{-1} \text{ cm}^{-1}$)	Quantum yield	Brightness ^a			Lifetime (ns)		
			$\epsilon \times \text{QY}$	PCH	<i>In vivo</i>	τ_{bleach}^b	τ_{ϕ}	τ_M
mTurquoise	30 (434 ^c)	0.84 (474 ^d)	25	1.5	129	1.5	3.7	3.8
mTurquoise-GL	27	0.82 (475 ^d)	22	1.5	127	1.0	3.9	4.1
mTurquoise-DR	10	0.93	9	1.4	57	1.8	4.2	4.4
mTurquoise-GV	23	0.82	19	1.6	120	0.8	3.9	4.0
mTurquoise-RA	23	0.47 (473 ^d)	11	0.8	69	1.8	2.3	2.5
SCFP3A ^e	30	0.56	17	1.0	100	1.0	2.7	3.2
mCerulean ^e	33	0.49	16	0.7	87	1.2	2.3	3.1
ECFP ^e	28	0.36	10	0.6	59	n.a.	2.3	3.0

^aBrightness was determined as the intrinsic molecular brightness of purified protein ($\epsilon \times$ quantum yield (QY)), from photon-counting histogram (PCH) analysis (relative to SCFP3A) and upon expression *in vivo* in HeLa cells (relative to SCFP3A). ^bTime needed to bleach 1/e of total fluorescence relative to SCFP3A (higher numbers reflect higher photostability). ^cAbsorbance maximum (nm). ^dEmission maximum (nm). ^eValues from ref. 4.

We constructed a library in which the codon encoding Thr65 of SCFP3A (ref. 4) was randomized by using a primer with a degenerate codon NNM (N is any nucleotide and M is A or C; Online Methods). We observed substantial differences in the fluorescence lifetimes for different colonies (Fig. 1a). Many colonies displayed a reduced lifetime but at least three had a notably higher fluorescence lifetime ($\tau_{\phi} > 3.5$ ns) than that of SCFP3A. Sequencing of clones revealed mutants encoding SCFP3A with a single amino acid change at position 65 from a threonine to a serine or tyrosine. As transfection of the plasmid encoding SCFP3A (T65Y) did not yield fluorescent mammalian cells, we did not analyze this variant further. We picked three clones with a lower lifetime ($\tau_{\phi} < 2.5$ ns), and these encoded T65G, T65C and T65N variants. Notably, the T65C and T65N mutants had slightly red-shifted spectra (data not shown).

When expressed in mammalian cells, SCFP3A (T65S), which we named mTurquoise, had a measured phase and modulation fluorescence lifetime of 3.7 ns. The similarity between phase and modulation lifetime provides strong evidence for mono-exponential fluorescence decay. This is in stark contrast to data for SCFP3A and Cerulean for which the modulation lifetime is substantially higher than the phase lifetime, as a consequence of multiexponential decay⁴. Thorough characterization of the fluorescence lifetime in living mammalian cells by multifrequency fluorescence lifetime imaging microscopy (FLIM) demonstrated that mTurquoise has a mono-exponential lifetime of 3.78 ns (Supplementary Data). In agreement with the increased lifetime, the quantum yield of mTurquoise was 0.84, 1.5-fold greater than that of SCFP3A (Table 1). As the extinction coefficients of mTurquoise and SCFP3A were similar, this indicates a 50% increase of the intrinsic molecular brightness of mTurquoise as compared to that of SCFP3A. Also, the photostability of mTurquoise was greater than that of mCerulean or SCFP3A. The mTurquoise pK_a of 4.5 was similar to that of SCFP3A (data not shown).

To examine the use of mTurquoise for localization studies, we made N- and C-terminal fusion proteins with an actin-binding peptide and with α -tubulin and expressed them in HeLa cells. These fusion proteins localized to the actin cytoskeleton or microtubules, as expected (Supplementary Fig. 2). Owing to the improved quantum yield, the calculated Förster radius (R_0) value for the mTurquoise-mVenus FRET pair was 4 Å greater than that for SCFP3A-mVenus, 57 Å, and similar to that for the EGFP-tagRFP FRET pair⁷. To evaluate the use of mTurquoise as a FRET donor in cells, we expressed an mTurquoise-mVenus(L68V) fusion protein, which we compared to mCerulean-mVenus(L68V) and SCFP3A-mVenus(L68V). Fluorescence lifetime imaging demonstrated an increased FRET efficiency and a much higher lifetime

contrast for mTurquoise as FRET donor (Table 2). Emission spectra of the same constructs, normalized to the directly excited yellow fluorescence signal from mVenus(L68V) (Fig. 1b), demonstrated 1.5-fold greater cyan fluorescence signal and an increased yellow-sensitized emission for the mTurquoise-mVenus(L68V) construct, implying improved signal-to-noise ratio for ratiometric FRET sensors containing mTurquoise for both cyan and yellow fluorescence channels.

Next, we performed a combined multi-site-directed saturation mutagenesis on mTurquoise Asp148 and Val224, as these positions are known to affect fluorescent protein brightness^{5,8,9}. Variants with the mutations D148G, V224L (mTurquoise-GL), V224R (mTurquoise-DR) and D148G (mTurquoise-GV) had increased fluorescence lifetimes of greater than 4 ns. Mutations V224L and V224R have been found previously to improve brightness of blue⁸ and yellow fluorescent proteins⁹. The lifetime values of these variants are among the highest reported for fluorescent protein variants thus far.

Additionally, we screened for variants with intermediate fluorescence lifetimes for which the phase (τ_{ϕ}) and modulation (τ_M) lifetimes were similar for lifetime unmixing. We identified two variants with lifetimes of around 2.5 ns, and sequencing revealed that those variants had the mutations D148S, V224Q and D148R, V224A (mTurquoise-RA). Emission spectra of mTurquoise and mTurquoise-RA (Fig. 1c) were the same, but that of the D148S, V224Q variant was different (data not shown).

The extinction coefficients for some of the new cyan fluorescent protein variants were notably lower compared to values obtained for SCFP3A. As we determined the extinction coefficient using protein purified from *Escherichia coli*, we hypothesized that for some variants poor maturation caused a reduction in extinction coefficients. To address this issue, we used fluorescence fluctuation spectroscopy, as it only detects the fluorescing and hence mature proteins. We used photon-counting histogram analysis to determine the molecular brightness¹⁰ of the variants. Compared to the molecular brightness of SCFP3A (normalized to 1) mTurquoise had a 50% improved brightness, which agrees with improvement of the intrinsic molecular brightness. The molecular brightness of the other variants also closely matched the measured quantum yields, indicating that all the mature cyan fluorescent protein species have similar extinction coefficients. Subsequently, we examined whether the improved brightness was also observed in cells. First, we measured maturation in *E. coli* (Supplementary Fig. 3), which revealed strongly increased fluorescence of bacteria expressing mTurquoise and mTurquoise-GL as compared to SCFP3A

Table 2 | FRET efficiency determined by FLIM

Donor	Acceptor	R_0 (Å) ^a	τ_D (ns) ^b	τ_{DA} (ns) ^c	$\Delta\tau$ (ns) ^d	E (%) ^e
mCerulean	mVenus(L68V)	52.4	2.44 ± 0.03 ($n = 32$)	1.81 ± 0.04 ($n = 42$)	0.63 ± 0.07	26 ± 3
SCFP3A	mVenus(L68V)	53.6	2.83 ± 0.06 ($n = 33$)	2.01 ± 0.06 ($n = 36$)	0.82 ± 0.11	29 ± 4
mTurquoise	mVenus(L68V)	57.3	3.66 ± 0.06 ($n = 36$)	2.44 ± 0.10 ($n = 34$)	1.22 ± 0.15	33 ± 4

^aFörster radius. ^bPhase lifetime of the donor in absence of acceptor. ^cPhase lifetime of the donor in presence of the acceptor. ^dLifetime contrast ($\tau_D - \tau_{DA}$). ^eFRET efficiency calculated according to $(1 - (\tau_{DA}/\tau_D)) \times 100\%$.

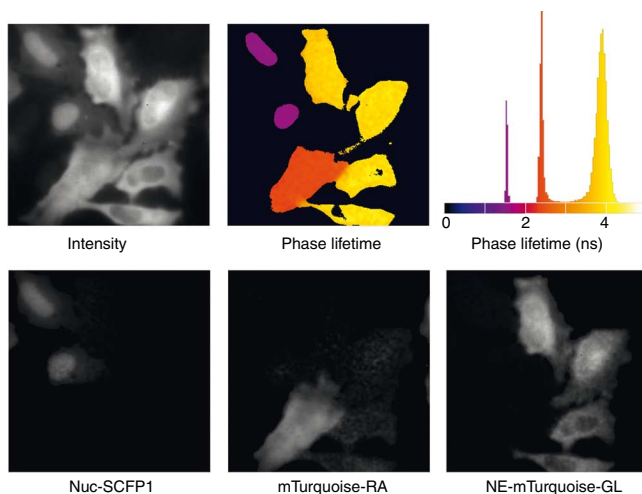


Figure 2 | Three-component lifetime unmixing of cyan fluorescent protein variants from a single (frequency) FLIM experiment. HeLa cells were transfected separately to express either SCFP1 with a nuclear import signal (nuc-SCFP1), mTurquoise-RA or mTurquoise-GL with a nuclear export signal (NE-mTurquoise-GL) and were mixed the next day. The phase lifetime map and lifetime histogram show the three distinct species. The respective contribution to the steady-state cyan fluorescence was unmixed and the cyan fluorescence images of the individual components are shown at the bottom. Image width, 100 μm .

analysis of populations displaying FRET for the first time with a cyan fluorescent protein variant as donor, using frequency domain FLIM with global analysis¹⁴ or using time domain FLIM with bi-exponential decay analysis¹⁵. Because of its increased brightness and lifetime, mTurquoise is the preferred cyan variant for fluorescence imaging and FRET studies in combination with yellow fluorescent protein.

METHODS

Methods and any associated references are available in the online version of the paper at <http://www.nature.com/naturemethods/>.

Note: Supplementary information is available on the Nature Methods website.

ACKNOWLEDGMENTS

We thank I. Elzenaar and M. Adjobo-Hermans for pilot experiments on the 2A co-expression assay and the members of our laboratory for encouraging discussions, J.E.M. Vermeer (University of Amsterdam) for providing plasmid encoding peroxi-YFP with a C-terminal SKL peroxisomal targeting sequence and E.L. Snapp (Albert Einstein College of Medicine) for providing plasmid encoding ER-tdTomato. Part of this work is supported by the EU integrated project on 'Molecular Imaging' (LSHG-CT-2003-503259).

AUTHOR CONTRIBUTIONS

J.G. and T.W.J.G. designed research; J.G., L.v.W., M.A.H., K.J. and T.W.J.G. conducted experiments; J.G., L.v.W., M.A.H., N.O.E.V. and T.W.J.G. analyzed data; and J.G. and T.W.J.G. wrote the paper.

COMPETING INTERESTS STATEMENT

The authors declare no competing financial interests.

Published online at <http://www.nature.com/naturemethods/>.

Reprints and permissions information is available online at <http://npg.nature.com/reprintsandpermissions/>.

or mCerulean and a 1 h delayed maturation of mTurquoise in bacteria. In contrast, the variant mTurquoise-DR was hardly fluorescent, which agreed with the observed poor extinction coefficient resulting from incomplete maturation (**Supplementary Data**). Next, we quantified brightness in eukaryotic cells using an assay in which the cyan fluorescence was corrected for the respective protein expression level (determined by transfection efficiency), by quantitative coexpression of the yellow fluorescent protein variant mVenus(L68V): the proteins were separated by a 2A viral peptide sequence that prevents peptide bond formation, effectively expressing two separate proteins at an equimolar ratio¹¹. By acquiring the fluorescence intensity of all cyan fluorescent protein variants relative to mVenus(L68V) fluorescence, the brightness of the cyan fluorescent protein variants (the product of intrinsic molecular brightness and maturation efficiency) in living cells can be directly compared (**Supplementary Fig. 4**). Overall, the cellular brightness (**Table 1**) correlated very well with measured quantum yields and intrinsic molecular brightness. mTurquoise-DR was the exception with a rather poor cellular brightness, owing to reduced maturation in mammalian cells similar to what we observed in *E. coli*. The cellular brightness of mTurquoise was ~1.3- and 1.5-fold higher than that of SCFP3A and mCerulean, respectively.

The fluorescence lifetime variants mTurquoise-RA and mTurquoise-GL together with a previously reported variant, SCFP1, enabled lifetime unmixing of three variants. Triple lifetime unmixing requires three species of which the lifetimes are arranged in a triangular fashion in the polar plot^{12,13} (**Supplementary Data** and **Supplementary Fig. 5**). To determine whether triple lifetime unmixing can be applied to lifetime variants that are spectrally identical, we mixed cells transfected with plasmids encoding SCFP1 or mTurquoise-RA or mTurquoise-GL and discerned the three expected lifetimes (**Fig. 2**). Because fluorescence lifetimes and fluorescence spectra are orthogonal spectroscopic parameters, triple lifetime unmixing can be combined with multicolor imaging, thereby expanding multiparameter imaging applications (**Supplementary Data** and **Supplementary Fig. 6**).

Our results demonstrate that screening based on excited state lifetime is a powerful means of identifying autofluorescent proteins variants with improved quantum yield and altered fluorescence decay properties. The mono-exponential decay (**Supplementary Data**) of mTurquoise will enable quantitative

1. Heim, R. & Tsien, R.Y. *Curr. Biol.* **6**, 178–182 (1996).
2. Chudakov, D.M., Lukyanov, S. & Lukyanov, K.A. *Trends Biotechnol.* **23**, 605–613 (2005).
3. Miyawaki, A. *Dev. Cell* **4**, 295–305 (2003).
4. Kremers, G.J., Goedhart, J., van Munster, E.B. & Gadella, T.W. Jr. *Biochemistry* **45**, 6570–6580 (2006).
5. Rizzo, M.A., Springer, G.H., Granada, B. & Piston, D.W. *Nat. Biotechnol.* **22**, 445–449 (2004).
6. van Munster, E.B. & Gadella, T.W. *Adv. Biochem. Eng. Biotechnol.* **95**, 143–175 (2005).
7. Merzlyak, E.M. *et al. Nat. Methods* **4**, 555–557 (2007).
8. Mena, M.A., Treynor, T.P., Mayo, S.L. & Daugherty, P.S. *Nat. Biotechnol.* **24**, 1569–1571 (2006).
9. Nguyen, A.W. & Daugherty, P.S. *Nat. Biotechnol.* **23**, 355–360 (2005).
10. Chen, Y., Muller, J.D., So, P.T. & Gratton, E. *Biophys. J.* **77**, 553–567 (1999).
11. Szymczak, A.L. *et al. Nat. Biotechnol.* **22**, 589–594 (2004).
12. Digman, M.A., Caiolfa, V.R., Zama, M. & Gratton, E. *Biophys. J.* **94**, L14–L16 (2008).
13. Pepperkok, R., Squire, A., Geley, S. & Bastiaens, P.I. *Curr. Biol.* **9**, 269–272 (1999).
14. Verveer, P.J., Wouters, F.S., Reynolds, A.R. & Bastiaens, P.I. *Science* **290**, 1567–1570 (2000).
15. Yasuda, R. *et al. Nat. Neurosci.* **9**, 283–291 (2006).



ONLINE METHODS

Mutagenesis. pRSET-SCFP3A⁴ was used as a template for lifetime screening. Site-directed saturation mutagenesis of the codon encoding amino acid at SCFP3A position 65 was performed using the 65X-forward primer and 65X-reverse primer (primers are listed in **Supplementary Table 1**). After cutting the product with DpnI (Fermentas), BL21(DE3) bacteria were transformed with the ligated plasmids and plated. For simultaneous mutagenesis at SCFP3A positions 148 and 224 we used the QuikChange Multi Site-Directed Mutagenesis kit (Stratagene) with the 148X and 224X primer. The library was transformed into XL-10 gold cells. Plasmid DNA was isolated and retransformed into BL21(DE3) bacteria. Plates with colonies of BL21(DE3) bacteria were used for lifetime screening. DNA isolated from BL21(DE3) colonies was purified and used for sequencing. Proteins tagged with histidine tags were isolated using His-Bind resin (Novagen). Subsequent protein purification by fast protein liquid chromatography (FPLC) and spectroscopic characterization were performed as described previously⁴.

Fluorescence lifetime imaging microscopy (FLIM) screen. FLIM experiments and subsequent image analysis were essentially performed as described⁷. A 440 nm modulated diode laser (LDH-M-C-440; PicoQuant) was intensity-modulated at a frequency of 75.1 MHz. The light was reflected by a 455DCLP dichroic mirror and the cyan fluorescent protein emission was passed through a D480/40 band-pass emission filter (Chroma Technology). Emission was detected using a radio frequency (RF)-modulated image intensifier (Lambert Instruments II18MD) coupled to a charge-coupled device (CCD) camera (Photometrics HQ) as detector. For yellow fluorescent protein and tandem dimer (td)Tomato dual-color imaging (**Fig. 2b**), yellow fluorescence was detected using a Chroma HQ500/20 nm excitation filter, a Chroma 525DCXR dichroic mirror and a Semrock FF01-542/27 nm emission filter; and tdTomato fluorescence was detected using a Chroma D577/20 nm excitation filter, a Chroma 600DCXR dichroic mirror and a Chroma HQ630/60 nm emission filter and a 100 W Hg lamp as excitation source.

The objective was replaced by a FL 800 mm lens (Melles-Griot) for fluorescence lifetime screening of Petri dishes with fluorescent colonies. A tube on top of which a Petri dish could be fitted (diameter, 100 mm; and length, 760 mm) was mounted on the stage (**Supplementary Fig. 1**).

Constructs. For expression in eukaryotic cells, the genes encoding cyan fluorescent protein variants were cut from a modified RSET plasmid with AgeI and BsrGI and inserted in the Clontech-like C1 and N1 vector using the same enzymes. The gene encoding LifeAct-mTurquoise was made by inserting the oligonucleotide linkers LifeAct-forward and LifeAct-reverse encoding the LifeAct sequence¹⁶ into a pmTurquoise-N1 vector using EcoRI and BamHI restriction sites. The gene encoding mTurquoise- α -tubulin was made by replacing the *tagRFP* gene with *mTurquoise* gene in the tagRFP- α -tubulin construct⁷. The genes encoding mVenus(L68V)-mTurquoise and mVenus(L68V)-mCerulean fusion constructs were made by replacing the *SCFP3A* gene in the construct encoding the mVenus(L68V)-SCFP3A fusion⁴.

SCFP1 carrying a nuclear localization signal (nuc-SCFP1) and SCFP3A carrying a nuclear export signal (ne-SCFP3A) have

been described previously⁴. The cyan fluorescent protein gene was exchanged for mTurquoise variant genes by using AgeI and BsrGI restriction sites.

Plasmids encoding cyan fluorescent protein-2A-yellow fluorescent protein for equimolar expression of the two proteins (CFP-2A-YFP plasmid) were constructed by adding the 2A peptide sequence to the cyan fluorescent protein cDNA by PCR with the 2A-forward primer and two reverse primers 2A-rev1 and 2A-rev2 in a molar ratio of 1:10. The PCR product was cut with NheI and BamHI and introduced into a Clontech-like C1 vector cut with the same enzymes. Next, mVenus(L68V) was amplified by using the FP-BamHI-fwd and FP-BamHI-rev primers. PCR product digested with BamHI was ligated into the vector digested with BamHI.

To change the cyan fluorescent protein variant, the CFP-2A-YFP plasmid was partially digested with NheI and BsrGI to remove cyan fluorescent protein. Another cyan fluorescent protein variant was cut with NheI and BsrGI from a Clontech-like C1 plasmid and ligated into the vector. All plasmids were verified by sequencing.

Relative brightness in eukaryotes. HeLa cells were transfected with CFP-2A-YFP plasmids that drive expression of CFP and YFP at equal level. Subsequently images of cyan and yellow fluorescent protein-expressing cells were acquired at 37 °C by a Zeiss 200M inverted fluorescence microscope equipped with a 40 \times Plan-Neofluar (1.3 NA) oil-immersion lens (Zeiss). The set-up was controlled by MetaMorph software (Molecular Devices). Excitation light from a Cairn Xenon Arc lamp was selected by a monochromator (Cairn Research). For cyan fluorescent protein, 420 nm excitation light (slit 30 nm) was reflected by a 455DCLP dichroic mirror, and emission was passed through a 470/30 nm bandpass filter. In case of yellow fluorescent proteins, 500 nm excitation light (slit 30 nm) was reflected by a 515DCXR dichroic mirror and the fluorescence was passed through a 535/30 nm band-pass filter. Images were acquired with a Photometrics CoolSnap HQ CCD camera with 4 \times 4 binning. All images were background- and flatfield-corrected. The average fluorescence intensity of individual cells was measured using the ObjectJ plugin (<http://simon.bio.uva.nl/objectj/>) for ImageJ.

Multifrequency FLIM. Phase shift and demodulation were determined at 10 logarithmically spaced frequencies (10.0, 14.3, 20.5, 29.3, 41.9, 59.8, 85.5, 122.3, 174.9 and 250.0 MHz). At each frequency a FLIM stack was acquired with 18 images (2 \times 2 binning) with an exposure time of 100 ms. All data were background-corrected. The average of three measurements (at least 2 cells per measurement) were used for the fit. Fits were performed with freely available software (<http://cfs.umbi.umd.edu/cfs/software/index.html>) from the center for fluorescence spectroscopy (University of Maryland School of Medicine). As an internal control, the monoexponential lifetime of mTFP1 was used.

Spectral imaging microscopy. Spectral imaging of living cells was performed as described¹⁷ 2 d after transfection using an imaging spectrograph-CCD detector and 436/10 nm excitation, an 80/20 (transmission/reflection) dichroic and LP460 filtered fluorescence. To acquire yellow fluorescence, a spectral image was taken under identical conditions, except for the excitation at 500/20 and

emission detected at 532/20 nm. Each spectral image was normalized to direct excited yellow fluorescent protein fluorescence to correct for differences in protein expression.

Fluorescence fluctuation spectroscopy. Protein samples were diluted into 10 mM Tris (pH 8.0) supplemented with 0.2% BSA to a final concentration of around 50 nM. Fluorescence fluctuation spectroscopy (FFS) was performed on a Leica SP5 confocal setup. A 63× water immersion objective (numerical aperture (NA) 1.2) was used. The samples were excited using a 440 nm diode laser and the emission was filtered through a LP460 nm filter. The emission light passed a size-adjustable pinhole, set at 1 Airy unit, and was guided via an optical fiber into an avalanche photodiode. One million photons were collected using an ISS photon-counting card and analyzed in SSTC FFS Dataprocessor v.2.1. The data was binned to time windows of 0.2 μs (for FCS) or 1, 5, 10, 100 and 1,000 μs (for photon-counting histogram (PCH)) and auto-correlated or plotted as a photon counting histogram. The FCS curve was fitted with a three-dimensional Brownian diffusion model including dark-state kinetics¹⁸, and the PCH curves were analyzed with a two-component three-dimensional PCH model containing corrections for dark-state kinetics, diffusion and the non-Gaussian detection volume¹⁹. The molecular brightness of the first component was fixed to the value obtained in the control measurement consisting of 10 mM Tris buffer with 0.2% BSA, using a one-component fitting model. FCS and PCH curves were fitted simultaneously in which parameters as dark-state relaxation time, diffusion time, volume structure parameter, particle number and molecular brightness were globally linked.

Three-component lifetime unmixing. For frequency domain FLIM, the fluorescence lifetime can be measured from the phase shift (φ) and demodulation (M) of the fluorescence emission with respect to the excitation light. From each of these observables, no matter how complex the actual excited state deactivation kinetics, an average fluorescence lifetime (τ_φ and τ_M , respectively) can be determined according to equation 1 in which ω is the angular frequency of modulation ($\omega = 2\pi f$).

$$\begin{cases} \tau_\varphi = \frac{1}{\omega} \frac{S}{G} \\ \tau_M = \frac{1}{\omega} \sqrt{\frac{1}{S^2 + G^2} - 1} \end{cases} \quad \text{with} \quad \begin{cases} S = M \sin \varphi \\ G = M \cos \varphi \end{cases} \quad (1)$$

S and G are the polar phase and modulation coordinates. If the excited state decay is composed of n single exponentially decaying components of which the i^{th} component has a fluorescence lifetime τ_i and a fractional amplitude a_i (and fractional contribution to the steady state fluorescence α_i), then it can be proved that:

$$\begin{cases} S = \sum_{i=1}^n \frac{\alpha_i \omega \tau_i}{1 + \omega^2 \tau_i^2} \\ G = \sum_{i=1}^n \frac{\alpha_i}{1 + \omega^2 \tau_i^2} \end{cases} \quad \text{with} \quad \alpha_i \equiv a_i \tau_i / \sum_{i=1}^n a_i \tau_i \quad (2)$$

For a single decaying fluorophore ($n = 1$) it can be shown that $\tau_\varphi = \tau_M = \tau$ and for multiexponential decaying fluorophores

$\tau_\varphi < \tau_M$. By close inspection of equation 2, it can be inferred that both S and G are linear with respect to fractional (steady state fluorescence) contribution, but with different weight factors only depending on the fluorescence lifetime of that component. Hence, if we have a mixture of m multi-exponentially decaying species, where the fractional contribution of species j to the steady state fluorescence is f_j (with $\sum f_j = 1$), then equation 2 can be rewritten as:

$$\begin{cases} S = \sum_{j=1}^m f_j S_j \\ G = \sum_{j=1}^m f_j G_j \end{cases} \quad \text{with} \quad \begin{cases} S_j = \sum_{i=1}^{n_j} \frac{\alpha_{ij} \omega \tau_{ij}}{1 + \omega^2 \tau_{ij}^2} \\ G_j = \sum_{i=1}^{n_j} \frac{\alpha_{ij}}{1 + \omega^2 \tau_{ij}^2} \end{cases} \quad (3)$$

Hence, if we know S_j and G_j , that is, the phase and modulation of each multiexponentially decaying species (irrespective of the complexity of their decay), S and G of the complex mixture is only dependent on the fractional abundance of each species in a linear way. In case of three complex species (each with a single or multiexponential decay) this problem is determined as we have two observables (φ and M , that is, S and G) and two unknowns: f_1 and f_2 , as $f_3 = 1 - f_1 - f_2$. Hence, for three species, the average lifetime parameters S and G from equation 3 can be 'lifetime unmixed' into the fractional contribution according to:

$$\begin{cases} f_1 = \frac{SG_2 - SG_3 + S_3G - S_2G + S_2G_3 - S_3G_2}{S_1G_2 - S_2G_1 + S_2G_3 - S_3G_2 + S_3G_1 - S_1G_3} \\ f_2 = \frac{SG_3 - SG_1 + S_1G - S_3G + S_3G_1 - S_1G_3}{S_1G_2 - S_2G_1 + S_2G_3 - S_3G_2 + S_3G_1 - S_1G_3} \\ f_3 = \frac{SG_1 - SG_2 + S_2G - S_1G + S_1G_2 - S_2G_1}{S_1G_2 - S_2G_1 + S_2G_3 - S_3G_2 + S_3G_1 - S_1G_3} \end{cases} \quad (4)$$

The advantage of the method is that once the average fluorescence lifetimes τ_φ and τ_M of each of the three complex decaying species at a particular modulation frequency ω are known, no extra calibration measurements are required since the τ_φ and τ_M lifetime values can be directly used for the unmixing procedure by using equation 1. Hence, no assumptions or experimental determination is required of the actual complex exponential decay components of each species before or during lifetime unmixing. In case of spectrally identical species with relative brightness q_j and local concentration c_j , it can be shown that $f_j = q_j c_j / \sum q_j c_j$. Hence, in that case the relative local concentration directly follows from the quantitative fractional species contribution f_j obtained by lifetime unmixing. Hence, by multiplying the detected steady state fluorescence intensity at each pixel with f_j / q_j , three images of the local concentration c_j of the three species are determined that can be quantitatively compared, that is, for local stoichiometry. The error estimation of the determined unmixed intensities is available in the **Supplementary Note**.

16. Riedl, J. *et al. Nat. Methods* **5**, 605–607 (2008).
17. Vermeer, J.E., Van Munster, E.B., Vischer, N.O. & Gadella, T.W. Jr. *J. Microsc.* **214**, 190–200 (2004).
18. Bacía, K. & Schwille, P. *Methods* **29**, 74–85 (2003).
19. Perroud, T.D., Huang, B. & Zare, R.N. *ChemPhysChem* **6**, 905–912 (2005).